

Cite this: DOI: 10.1039/c1sm05298e

www.rsc.org/softmatter

HIGHLIGHT

# Model systems for single molecule polymer dynamics

Folarin Latinwo<sup>a</sup> and Charles M. Schroeder<sup>\*ab</sup>

DOI: 10.1039/c1sm05298e

Double stranded DNA (dsDNA) has long served as a model system for single molecule polymer dynamics. However, dsDNA is a semiflexible polymer, and the structural rigidity of the DNA double helix gives rise to local molecular properties and chain dynamics that differ from flexible chains, including synthetic organic polymers. Recently, we developed single stranded DNA (ssDNA) as a new model system for single molecule studies of flexible polymer chains. In this work, we discuss model polymer systems in the context of “ideal” and “real” chain behavior considering thermal blobs, tension blobs, hydrodynamic drag and force–extension relations. In addition, we present monomer aspect ratio as a key parameter describing chain conformation and dynamics, and we derive dynamical scaling relations in terms of this molecular-level parameter. We show that asymmetric Kuhn segments can suppress monomer–monomer interactions, thereby altering global chain dynamics. Finally, we discuss ssDNA in the context of a new model system for single molecule polymer dynamics. Overall, we anticipate that future single polymer studies of flexible chains will reveal new insight into the dynamic behavior of “real” polymers, which will highlight the importance of molecular individualism and the prevalence of non-linear phenomena.

## 1 Introduction

Over the last few years, double stranded DNA (dsDNA) has served as a model system for single molecule polymer dynamics. Single polymer studies of dsDNA have been used to probe the equilibrium and non-equilibrium dynamics of polymer chains in solution.<sup>1</sup> In particular, bacteriophage lambda DNA ( $\lambda$ -DNA) has been extensively used to study chain dynamics using fluorescence microscopy, and experimental results have been complemented by Brownian dynamics simulation. Single molecule polymer studies enable direct and real-time observation of polymer backbone dynamics and allow for characterization of molecular subpopulations.

Using this approach, a wide range of static and dynamic polymer phenomena has been studied using fluorescently-labeled dsDNA as a model system, including the coil–globule transition,<sup>2</sup> polymer relaxation,<sup>3</sup> stretching in uniform flow,<sup>4</sup> scaling of diffusion coefficients,<sup>5</sup> dynamics in extensional<sup>6,7</sup> and shear flow,<sup>8</sup> polymer conformation hysteresis,<sup>9</sup> and more recently, polymer dynamics in confined geometries<sup>10,11</sup> and concentrated polymer solutions.<sup>12,13</sup> In addition, single polymer observation has been used to uncover the existence of variable stretching pathways and distinct molecular conformations for polymers unraveling in flow termed “molecular individualism”.<sup>14</sup>

Overall, dsDNA is a convenient model system for studying polymer dynamics. Experimentally, sample preparation and fluorescent labeling of dsDNA are straightforward and monodisperse samples of  $\lambda$ -DNA are available, which simplifies data analysis. In addition, dsDNA is an aqueous-based polymer

system that can be studied using optically-pure biological buffers, thereby facilitating fluorescence imaging. Due to the double helix structure, dsDNA is a semiflexible polymer chain with a relatively rigid backbone. However, the vast majority of synthetic organic polymer chains are flexible polymers with single carbon–carbon bonds forming chain linkages along the backbone of the macromolecule. Clearly, the local physical and chemical properties of dsDNA are distinct from common synthetic organic polymer chains.

Recently, we reported a new system for single molecule polymer studies based on single stranded DNA (ssDNA).<sup>15</sup> ssDNA is a flexible polymer with local physical properties similar to synthetic organic polymer chains. We developed a biochemical synthesis method for generating long contour length ssDNA molecules *via* rolling circle replication, which enables direct control of ssDNA sequence to prevent base pairing interactions and hairpin formation.<sup>15</sup> Using this

<sup>a</sup>Department of Chemical & Biomolecular Engineering, University of Illinois at Urbana–Champaign, UrbanaIL, 61801, USA. E-mail: cms@illinois.edu

<sup>b</sup>Center for Biophysics and Computational Biology, University of Illinois at Urbana–Champaign, UrbanaIL, USA

method, ssDNA chains are readily labeled with fluorescent dyes along the polymer backbone by incorporating chemically-modified nucleotides in a co-polymerization reaction during synthesis. Alternative strategies for generating ssDNA include thermal or chemical denaturation of dsDNA; however, fluorescent labeling of polymer backbones and control of ssDNA sequence are not easily achieved using these approaches. From a broad perspective, ssDNA opens the field of single polymer studies to a new class of macromolecules and provides a new system for direct observation of flexible chain dynamics.

In this article, we discuss the relationship between global chain properties and local chain chemistry, and we explore the impact of local properties on chain dynamics. Is the dynamic behavior of dsDNA characteristic of a universal class of truly flexible polymer chains, particularly in the context of de Gennes' dynamical scaling laws, which are developed for flexible polymer chains? What are the implications for real *versus* ideal chain behavior in the context of polymer dynamics? In this Highlight article, we consider the role of local polymer chemistry on universal scaling laws used to describe the dynamics of a large class of polymer chains.

## 2 Global versus local chain properties

In his classic text on polymer physics,<sup>16</sup> de Gennes develops universal scaling laws for polymer chains. Scaling relations are developed using a global view of polymers such that physical phenomena depend on global properties, such as chain length or concentration, but are independent of local chemical details, such as chemical identity, structure of side groups or bond rotations. Although universally applied to all polymers, de Gennes' scaling relations are developed for "model" flexible chains. In this section, we consider the chemical basis of chain flexibility and the implications for dynamics.

### 2.1 Flexibility

What determines chain flexibility? *Local flexibility* is determined by the molecular structure and chemical composition of

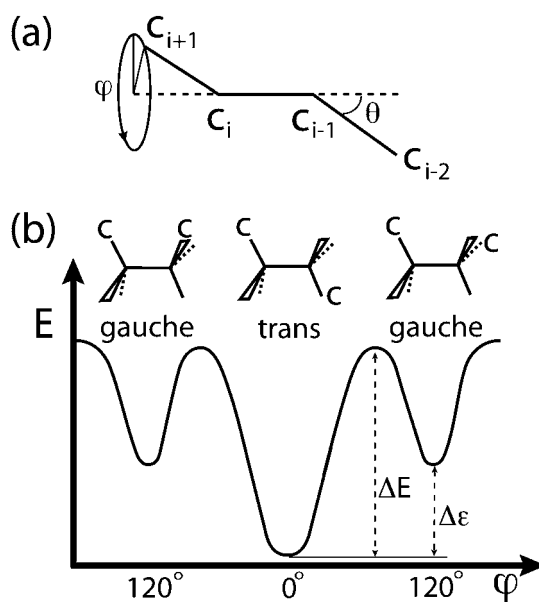


**Fig. 1** Local flexibility is determined by molecular structure. Hydrocarbon chain flexibility arises due to bond rotations. (a) Bond torsion and tetrahedral angles. (b) Polymer chain conformation energy.

a polymer chain.<sup>16,17</sup> Consider a hydrocarbon chain from a local viewpoint as shown in Fig. 1. Chain flexibility arises due to bond rotations about the torsion angles  $\varphi$ , whereas the tetrahedral angle  $\theta$  between carbon bonds is fixed at a nearly constant value. Chain conformation energy depends on the torsion angle  $\varphi$ , with three energy minima corresponding to a *trans* state ( $0^\circ$ ) and two *gauche* states ( $\pm 120^\circ$ ); in general, the *trans* state is the lowest energy conformation such that the carbon-carbon backbone lies in a plane (Fig. 1b).

*Static flexibility* is defined by the energy difference between *trans* (*t*) and *gauche* (*g*) states  $\Delta\epsilon$ , and for small values of the *t-g* energy difference  $\Delta\epsilon \approx kT$ , the *trans* and *gauche* states are equally preferred at thermal equilibrium. For example, polyethylene is extremely flexible in the static sense such that  $\Delta\epsilon \approx 0.8 kT$ . As  $\Delta\epsilon$  increases, the *trans* state is preferred and the chain becomes increasingly rigid.<sup>16</sup> *Dynamic flexibility* is determined by the energy barrier  $\Delta E$  between *trans* and *gauche* states, and for small values of the energy barrier  $\Delta E \approx kT$ , a chain is considered dynamically flexible, rapidly exploring many conformations without being "frozen" in a narrow subset of conformation space.

Flexibility mechanisms are fundamentally different for stiff polymers such as

dsDNA compared to hydrocarbon chains. Global chain conformation and local molecular structure for a hydrocarbon chain and dsDNA are shown in Fig. 2.

Due to the double helix structure, double stranded DNA is semiflexible and exhibits a uniform flexibility across the entire polymer backbone, which arises due to backbone contour fluctuations rather than torsion bond angle rotations in flexible chains.<sup>17</sup> Semiflexible polymers are described by the Kratky-Porod or worm-like chain model which is derived in the limit of small tetrahedral angles ( $\theta \rightarrow 0$ ) using a freely rotating chain model, thereby incorporating stiffness along the backbone. In this manner, a persistence length  $l_p$  may be defined such that:<sup>18</sup>

$$l_p \equiv \left\langle \frac{\vec{l}_1 \cdot \vec{R}}{l_1} \right\rangle \quad (1)$$

where  $l$  is the bond length,  $\vec{l}_1$  is the vector along the first bond and  $\vec{R}$  is the end-to-end vector. The persistence length is a measure of *local flexibility* and represents the distance along the backbone that must be traveled before bond vectors become uncorrelated. Double stranded DNA is locally stiff with a persistence length  $l_p \approx 53$  nm. In contrast, polyethylene is locally flexible with  $l_p \approx 0.57$  nm, two orders of magnitude smaller than  $l_p$  for dsDNA.<sup>19</sup> For flexible

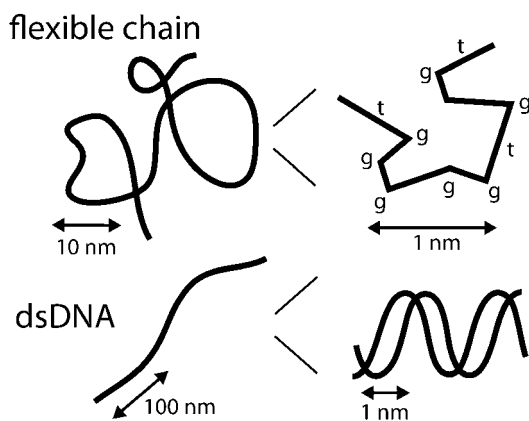


Fig. 2 Global chain conformations and local chemical composition for a flexible hydrocarbon chain and semiflexible dsDNA.

chains with torsion bond angles, the persistence length is a sensitive function of  $\Delta\epsilon$ , such that  $l_p$  increases rapidly with increasing  $\Delta\epsilon$ .

## 2.2 Global flexibility: implications for dynamics

De Gennes notes that dynamical scaling theories are derived for polymers under the assumption of static and dynamic flexibility “in the strongest form”.<sup>16</sup> Does this imply that scaling theories do not hold for semiflexible chains such as dsDNA? The answer is: not necessarily, and as for most questions in polymer science, depends on relative length scales. In the limit of a small persistence length  $l_p$  relative to the contour length  $L$  such that  $l_p \ll L$ , the chain will appear flexible over intermediate length scales larger than  $l_p$ . *Global flexibility* may be defined as the number of persistence lengths in a chain:

$$\frac{L}{l_p} \sim N \quad (2)$$

The global flexibility parameter scales as the number of statistical steps  $N$ . In general, chains with  $N > 100$  are considered globally flexible. Lambda DNA ( $L \approx 16.3 \mu\text{m}$ , 48502 bp) contains approximately 310 persistence lengths and has been considered flexible from a global perspective. However, the global flexibility argument does not preclude the possibility that local chain flexibility gives rise to distinct dynamics for flexible polymer chains due to excluded volume effects or intra-chain hydrodynamic

interactions, both of which depend on local backbone chemistry.

## 3 Chemical nature of model polymers: dsDNA & exible chains

The fundamental properties of real polymers differ markedly from ideal chains. Is dsDNA a real or ideal polymer chain? Here, we explore experimental evidence regarding real *versus* ideal chain behavior, with related implications on chain dynamics.

### 3.1 Real *versus* ideal chains

Ideal polymer chains are described by the absence of monomer–monomer interactions for monomers separated by many bonds along the backbone. In ideal chains, only *local correlations* between neighboring monomers are considered, which arise due to tetrahedral carbon–carbon bonds and steric hindrance between monomeric side groups.<sup>17,20</sup> Local constraints may be included by incorporating bond angle restrictions on the tetrahedral ( $\theta$ ) or torsion ( $\varphi$ ) angles as shown in Fig. 1. All ideal chains are described by a mean-square end-to-end distance:

$$\langle R^2 \rangle = C_\infty n l^2 \quad (3)$$

where  $C_\infty$  is the characteristic ratio,  $l$  is bond length and  $n$  is the number of backbone bonds. The overall effect of local constraints due to steric hindrance or bond angle restrictions is to increase the coil size ( $C_\infty > 1$ ), whereas an ideal chain with no constraints is called a freely-jointed chain and is described by a simple random walk of backbone bonds

( $C_\infty = 1$ ). Therefore, the absence of monomer–monomer interactions in ideal polymer chains yields a universal scaling of the average coil size with  $N$  such that  $R_0 \equiv \langle R^2 \rangle^{1/2} \sim \sqrt{N}$ . Typical values of the characteristic ratio are  $C_\infty \approx 5\text{--}9$  for flexible polymers.

Real polymer chains exhibit interactions between monomers separated by many bonds along the chain backbone. Physically, monomers interact by steric repulsion and generally exhibit attractions to nearby monomers or solvent molecules by van der Waals or additional intermolecular forces. In the case of a polyelectrolyte, charge–charge interactions between monomers lead to enhanced repulsion. Monomer interactions are modeled by an excluded volume  $v$ , which can be expressed as an integral of the Boltzmann weighted potential energy  $U(r)$  between two interacting monomers:

$$v = \int (1 - \exp[-U(r)/kT]) d^3r \quad (4)$$

In this manner, the excluded volume represents a net two-body interaction between monomer segments,<sup>17,21</sup> analogous to the second virial coefficient for non-ideal gases.<sup>22</sup> A net repulsion between monomers yields a positive excluded volume  $v > 0$ . Flory modeled “real chains” by balancing the steric repulsion energy between monomers due to excluded volume ( $v > 0$ ) with the entropy loss due to the swollen chain conformation. The Flory model provides an estimate of the coil size for a real chain:

$$R_F \approx v^{1/5} b^{2/5} N^{3/5} \quad (5)$$

where the Kuhn length  $b$  is defined as twice the persistence length  $b \equiv 2l_p$ . For spherical (symmetric) monomers with dimension  $b$ , the excluded volume is given by  $v \approx b^3$  in athermal solvents. For chains with positive excluded volume  $v > 0$ , Flory theory yields a universal scaling law for real chains such that  $R_F \approx bN^{3/5}$ . The Flory chain size may be expressed  $R_F = (\text{constant})bN^{3/5}$ , where the pre-factor is a strong function of the local chemical structure of the polymer chain and is not universal for all polymers.

### 3.2 Monomer aspect ratio: asymmetric monomers

Monomer aspect ratio is a key parameter describing the local asymmetry of the

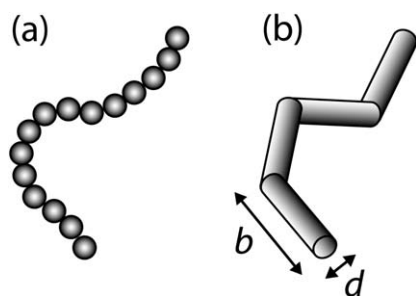


Fig. 3 Polymer chains with (a) symmetric and (b) asymmetric monomers.

polymer backbone and plays an important role in equilibrium and dynamic chain properties (Fig. 3).

The aspect ratio of a Kuhn monomer  $a$  is defined as the ratio of the Kuhn step size  $b$  to the chain diameter  $d$ :

$$a = \frac{b}{d} \quad (6)$$

In the case of spherical (symmetric) monomers with  $b \approx d$  in athermal solvents, the excluded volume  $v$  is modeled as a sphere such that  $v_{\text{sph}} \approx d^3 \approx b^3$ . For polymers with cylindrical (asymmetric) monomers, the occupied volume of a cylindrical monomer is  $v_o \approx bd^2$  and the excluded volume is  $v_{\text{cyl}} \approx b^2d$ , which is derived from a renormalization of the chain free energy density using a virial expansion.<sup>17</sup> Therefore, the ratio of excluded to occupied volume for a cylindrical monomer is the monomer aspect ratio:

$$\frac{v_{\text{cyl}}}{v_o} = a \quad (7)$$

Monomer aspect ratio is a local chain property that depends on the chemical structure of a polymer chain. Typical flexible chains have aspect ratios  $a \approx 2$ – $3$ , suggesting that the Kuhn step size is only a factor of 2 larger than the chain diameter for synthetic organic polymers. Molecular parameters for model polymer chains including dsDNA are shown in Table 1.†

The physical properties of dsDNA differ markedly from flexible polymer chains in many respects. Strikingly, the Kuhn segment aspect ratio for dsDNA is

† Parameters for dsDNA are given for DNA stained with intercalating dye YOYO-1 at an approximate dye:bp ratio of 1 : 4, commonly used in single polymer dynamics studies. The bare persistence length of ssDNA without electrostatic contributions is given.

$\approx 66$ , a factor of 55 larger than the aspect ratio for ssDNA and 33 times larger than  $a$  for polystyrene. dsDNA contains highly asymmetric monomers.

Monomer aspect ratio affects the properties of polymer chains in several ways. The swelling ratio of a polymer chain at equilibrium is defined as the ratio of the Flory chain size  $R_F$  to the size of an equivalent ideal chain  $R_o$ :

$$\frac{R_F}{R_o} \approx \left( \frac{v}{b^3} \sqrt{N} \right)^{1/5} \approx z^{1/5} \quad (8)$$

A chain interaction parameter  $z$  is defined such that:

$$z = \frac{v}{b^3} \sqrt{N} = \frac{\sqrt{N}}{a} \quad (9)$$

where the second equality results for asymmetric monomers with  $v = v_{\text{cyl}}$ . Excluded volume interactions swell chains for  $z > 1$ . The chain interaction parameter for  $\lambda$ -DNA ( $N \approx 150$ ) is  $z \approx 0.2$ , suggesting that excluded volume interactions are weak and the chain conformation for  $\lambda$ -DNA at equilibrium is nearly ideal. However, the chain interaction parameter for a long flexible polymer ( $N = 10^4$ ) with symmetric monomers is  $z \approx 50$  for polystyrene and  $z \approx 80$  for ssDNA, suggesting dominant monomer–monomer interactions, thereby resulting in swollen chains at equilibrium and real chain behavior. High aspect ratio monomers ( $a > \sqrt{N}$ ) suppress monomer–monomer interactions along the polymer chain backbone, thereby resulting in ideal chain conformations.‡

What are the implications of asymmetric monomers and ideal chain behavior on dynamics? High aspect ratio Kuhn segments effectively suppress monomer–monomer interactions, whereas dominant monomer interactions introduce non-linearities in polymer chain behavior, such as broadening of the relaxation time spectrum away from a simple mode picture.<sup>16</sup> Furthermore, dsDNA exhibits a relatively “open coil”, because the ratio of excluded to occupied volume *per monomer* is equal to the monomer aspect ratio  $v_{\text{cyl}}/v_o = a$ . From Flory theory, the number of monomer–monomer contacts *per chain* is estimated to be:

‡ See discussion of thermal blobs and self-diffusion coefficient for dsDNA.

$$\frac{vN^2}{R_F^3} \approx \left( \frac{v^2N}{b^6} \right)^{1/5} \approx \left( \frac{N}{a^2} \right)^{1/5} \quad (10)$$

As the monomer aspect ratio increases, the number of chain contacts decreases, which causes a concomitant increase in the average distance of contact per monomer. Therefore, polymer chains with large aspect ratio monomers exhibit increasingly free-draining coils compared to polymers with symmetric monomers. Free-draining polymer coils are hydrodynamically unshielded, which suppresses intramolecular hydrodynamic interactions in the coiled state.

Hydrodynamic interactions (HI) within a polymer play a key role in chain stretching dynamics. In the coiled state, monomers within a non-draining polymer are hydrodynamically shielded from an imposed flow field due to intrachain HI. However, monomers become fully exposed to a flow field in the stretched state, thereby resulting in an increase in hydrodynamic drag as a chain unravels in flow. The hydrodynamic drag ratio between the stretched (s) and coiled (c) conformations  $\zeta^s/\zeta^c$  is:<sup>23</sup>

$$\frac{\zeta^s}{\zeta^c} \approx \frac{2\pi L/\ln(L/d)}{kT/D} \approx \frac{L/\ln(L/d)}{R_F} \quad (11)$$

where the drag in the stretched state is given by slender body theory and the coil state drag is given by Zimm theory.<sup>24</sup> The drag ratio can be re-expressed using the Flory chain radius  $R_F$ :

$$\frac{\zeta^s}{\zeta^c} \approx \frac{(N^2a)^{1/5}}{\ln(Na)} \quad (12)$$

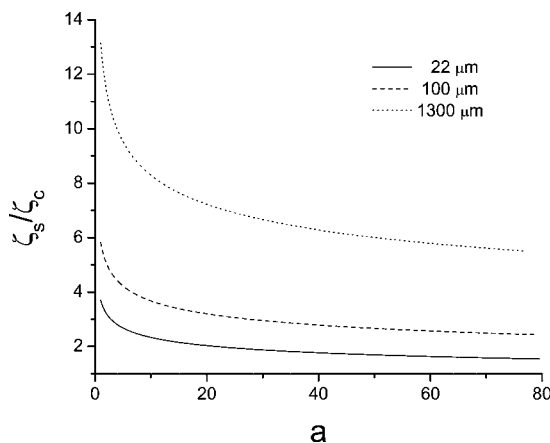
The quantity  $\zeta^s/\zeta^c$  given by eqn (12) is plotted in Fig. 4, where the drag ratio is considered for a polymer chain of constant contour length  $L$  as a function of increasing monomer aspect ratio  $a$ . As the monomer aspect ratio increases, the hydrodynamic drag ratio  $\zeta^s/\zeta^c$  decreases precipitously.§

§ In plotting the quantity  $\zeta^s/\zeta^c$  in Fig. 4, we included a numerical prefactor of order unity in order to match the scaling relation given by eqn (12) to more accurate estimates of drag using experimentally determined values of chain diffusivity  $D$ . In addition,  $\zeta^s/\zeta^c$  is plotted at constant  $L$  (not constant  $N$ ) by choosing a polymer molecular diameter  $d = 2$  nm.



**Table 1** Molecular parameters for common model polymer chains

Parameter	dsDNA	polystyrene	ssDNA
Aspect ratio of Kuhn segment, $a$	66	2	1.2
Kuhn step size, $b$ (nm)	132	1.5	1.2
Molecular diameter, $d$ (nm)	2.0	0.8	1.0
Thermal blob size, $\xi_T$ (nm)	8700	3.0	1.5

**Fig. 4** Chain hydrodynamic drag ratio as a function of Kuhn monomer aspect ratio  $a$  for chains of contour length  $L = 22, 100$  and  $1300 \mu\text{m}$ .

For most practical size dsDNA molecules, intrachain hydrodynamic interactions are weak, and the hydrodynamic drag ratio between the stretched and coiled conformations  $\zeta_s/\zeta_c$  is small. For  $\lambda$ -DNA, the hydrodynamic drag ratio is  $\zeta_s/\zeta_c \approx 1.6$ , calculated using accurate  $kT/D$  values rather than estimates from Zimm theory,<sup>9,25</sup> which suggests that intrachain hydrodynamic interactions are not dominant for  $\lambda$ -DNA. Indeed, Brownian dynamics simulations have verified that inclusion of hydrodynamic interactions is not required for quantitative modeling of  $\lambda$ -DNA chain dynamics.<sup>26,27</sup> For large dsDNA molecules, intrachain HI plays a role in dynamics. Hysteresis in polymer conformation arising due to intrachain HI was observed for dsDNA with contour length

$L = 1.3 \text{ mm}$  such that  $\zeta_s/\zeta_c \approx 5$ .<sup>9</sup> Conformation hysteresis is a striking manifestation of non-linear chain behavior, which is generally suppressed in polymer chains with high aspect ratio monomers.

### 3.3 Thermal blobs & real chains at equilibrium

In a real polymer, chain conformation is altered from the ideal chain conformation (Fig. 5). At equilibrium, monomers are in close contact within a polymer coil, and monomer–monomer interactions result in modified chain conformations on length scales larger than a thermal blob size  $\xi_T$ .

The length scale at which monomer interaction energy is comparable to thermal energy  $kT$  is defined as the *thermal blob* size  $\xi_T$  and is given by Flory theory:<sup>17</sup>

$$\xi_T \approx \frac{b^4}{v} \approx ab \quad (13)$$

The number of Kuhn steps in a thermal blob  $g_T$  is given by:

$$g_T \approx \frac{b^6}{v^2} \approx a^2 \quad (14)$$

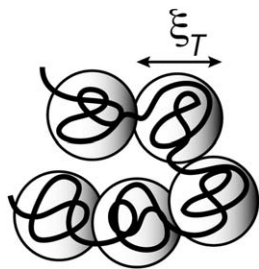
where the second equality arises in assuming asymmetric monomers with

excluded volume  $v_{\text{cyl}} = b^2d$  in an athermal solvent. For dsDNA, the number of Kuhn steps in a thermal blob is  $g_T = 4356$ , which is much larger than the number of Kuhn segments in  $\lambda$ -DNA ( $N = 150$ ). In addition, the thermal blob size for dsDNA is  $\xi_T = 8.7 \mu\text{m}$ , which is much larger than the coil size for  $\lambda$ -DNA at equilibrium  $R_g \approx 0.7 \mu\text{m}$ . Therefore, excluded volume interactions are weak for dsDNA chains of size  $\lambda$ -DNA, thereby resulting in nearly ideal chain behavior and no thermal blobs. Of course, these arguments are given for athermal solvents, where excluded volume is maximum, and consideration of solvent quality (*i.e.* less “good” solvents approaching  $\theta$  solvents) only further suppresses monomer interactions. As solvent quality approaches  $\theta$  conditions, the thermal blob size  $\xi_T$  increases.

How can these arguments be reconciled with experimental measurements of dsDNA coil diffusivity? The self-diffusion coefficient  $D$  of dsDNA was determined to follow the scaling law for polymer chains in good solvents with dominant excluded volume interactions such that  $D \sim N^{0.611}$  for dsDNA with contour lengths  $L$  ranging between  $2.0$  and  $140 \mu\text{m}$  ( $N = 15$  to  $1000$ ).<sup>5</sup> However, the thermal blob size for dsDNA is  $\xi_T = 8.7 \mu\text{m}$ , which is much larger than the coil size for  $\lambda$ -DNA. Within a thermal blob, the chain configuration is expected to follow ideal chain statistics such that  $R_o \sim N^{1/2}$ . Although dsDNA might exhibit a finite (albeit small) excluded volume  $v > 0$ , the chain interaction parameter  $z$  is expected to be less than unity for short dsDNA chains with  $N \approx 100$ – $1000$  (see above discussion on monomer symmetry). For polymer chains with  $z < 1$ , excluded volume interactions are weak and the universal scaling law for the Flory chain radius  $R_F \sim N^{3/5}$  in eqn (5) is not valid. From this perspective, the experimental results for dsDNA chain diffusivity are not well explained using thermal blob scaling arguments and chain statistics.

### 3.4 Pincus blobs & real chains under tension

A polymer chain can form *tension blobs*, also known as Pincus blobs, when exposed to an applied stretching force  $f$  (Fig. 6). On length scales smaller than the tension blob, the chain exhibits

**Fig. 5** Real chains form thermal blobs of size  $\xi_T$  at equilibrium due to excluded volume.

unperturbed dimensions in good solvents such that:

$$\xi \approx bg^{3/5} \quad (15)$$

where  $g$  is the number of Kuhn steps per blob. On length scales smaller than  $\xi$ , thermal energy creates an unperturbed chain conformation. On length scales larger than the tension blob, the chain conformation is perturbed beyond equilibrium due to the applied force  $f$ , and the chain begins to stretch in a preferred direction. Therefore, the free energy stored per blob is on the order of thermal energy  $kT$ , and the size of a tension blob  $\xi$  is given as the ratio of thermal energy to the chain stretching force such that:

$$\xi = \frac{kT}{f} \quad (16)$$

A stretching force  $f = 0.1$  pN yields tension blobs of size  $\xi = 41$  nm.

Due to the large Kuhn length  $b$ , dsDNA does not form tension blobs for most physically relevant forces ( $f > 0.1$  pN), where the Kuhn step size is larger than the tension blob  $b > \xi$ . However, at a stretching force of 0.1 pN, tension blobs in single stranded DNA contain approximately 40 Kuhn segments. Therefore, dsDNA does not form tension blobs for most physically realizable or practical chain tensions, and tension blobs do not play a major role in dsDNA chain stretching dynamics. However, flexible polymers such as ssDNA form tension blobs within a range of forces that directly impact chain stretching dynamics.

### 3.5 Force–extension: real versus ideal chains

For most synthetic polymers, chain elasticity has traditionally been modeled using the inverse Langevin chain (ILC) or Warner force–extension relations,<sup>20</sup> whereas the elasticity of semiflexible biopolymers such as dsDNA is well-described by the Marko–Siggia or

worm-like chain (WLC) force relation.<sup>28</sup> A common feature underlying all of these force relations is the assumption of ideal chain behavior and the absence of monomer interactions. A signature response of an ideal chain force relation (ILC, Warner, WLC) is a linear Hookean response at small extensions:

$$f \sim x/L \quad (\text{ideal}) \quad (17)$$

where  $x$  is chain extension. At large extensions, the linear regime is followed by a nonlinear response due to the finite extensibility of the polymer chain.

In contrast, the force–extension relation for real chains with dominant monomer interactions is markedly different compared to ideal chain models. In particular, the chain elasticity is *nonlinear* in the low force regime due to monomer interactions, thereby yielding:

$$f \sim (x/L)^{3/2} \quad (\text{real}) \quad (18)$$

The low-force, nonlinear force–extension relation was originally derived in 1976 by Pincus,<sup>29</sup> however, the nonlinear elasticity for real chains was only recently observed using ssDNA and a magnetic tweezer assay.<sup>30</sup> It is thought that the entire force–extension elastic relationship for real polymer chains consists of at least three regimes: (1) a linear regime at small coil perturbations ( $x \approx R_g$ ), where the force scaling is linear  $f \sim x/L$ , (2) a nonlinear (non-Hookean) regime predicted by Pincus to occur at low forces, such that  $f \sim (x/L)^{3/2}$ , and (3) a second nonlinear regime that arises due to the finite extensibility of the chain and occurs as the chain approaches its contour length ( $x/L \approx 1$ ). Finally, the existence of a fourth regime (located between the nonlinear Pincus regime and the nonlinear regime imposed by finite extensibility) has also been proposed.<sup>31</sup> The fourth regime is thought to occur because stronger forces lead to fewer monomers per Pincus blob, and excluded volume effects eventually become

unimportant at a length scale on the order of  $\xi_T$ . As the applied tension increases, Pincus blobs eventually contain less than 1 monomer, which might result in a change in the force–extension scaling relation (distinct from the Pincus scaling) if this regime is reached before a chain experiences its finite extensibility. However, this regime has not been experimentally observed, and further discussion is beyond the scope of this article.

## 4 Conclusions

The static and dynamic properties of *real* polymer chains differ markedly from *ideal* polymer chains due to monomer–monomer interactions. In many respects, dsDNA behaves as an ideal polymer chain, mainly due to a large Kuhn monomer aspect ratio  $a$ . Large monomer aspect ratios tend to inhibit monomer interactions, thereby suppressing nonlinear chain behavior, including the nonlinear low-force elasticity predicted by Pincus for flexible polymers in good solvents. Furthermore, intramolecular hydrodynamic interactions tend to be suppressed for polymers with asymmetric monomers, as reflected in small increases in hydrodynamic drag between coiled and stretched polymer conformations.

Recently, we introduced a new “model” system for single polymer experiments based on single stranded DNA.<sup>15</sup> Single stranded DNA is a flexible polymer chain with symmetric monomers in reasonable salt conditions. Flexible polymer chains with symmetric monomers ( $a \approx 1$ ) yield compact coils at equilibrium compared to dsDNA chains with equivalent contour length. In good solvents, flexible polymer chains tend to exhibit dominant monomer–monomer interactions which gives rise to “real” chain behavior. In addition, flexible polymers are highly extensible and more physically deformable compared to semiflexible polymers with asymmetric monomers. Therefore, we expect flexible chains such as ssDNA to show more pronounced non-linear and non-Newtonian flow properties compared to dsDNA, such as prominent polymer conformation hysteresis<sup>9</sup> and modified turbulent drag reduction.<sup>32,33</sup> Increased chain flexibility is expected to give rise to intriguing molecular conformations for deformed chains, including

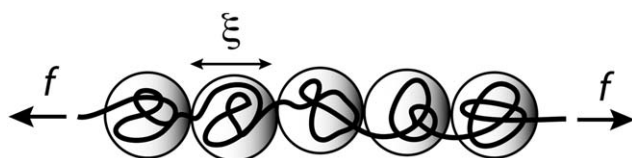


Fig. 6 Polymer chains form tension blobs of size  $\xi$  under a chain tension  $f$ .

kinks and knots along polymer chain backbones.<sup>16</sup> Indeed, many questions in the field remain to be explored using new polymeric systems, including the coil–globule phase transition for truly flexible polymers,<sup>2</sup> the nature of the coil–stretch transition for flexible chains,<sup>9</sup> polymer tumbling dynamics in shear flow,<sup>34</sup> and the dynamics of single flexible polymer chains under non-equilibrium conditions.<sup>20,21</sup> Single molecule polymer techniques appear to be extremely well-suited to address these questions in polymer science.

## Acknowledgements

This work was funded by an NIH Pathway to Independence Award, under Grant No. 4R00HG004183-04.

## References

- 1 E. S. G. Shaqfeh, *J. Non-Newtonian Fluid Mech.*, 2005, **130**, 1–28.
- 2 K. Yoshikawa, M. Takahashi, V. V. Vasilevskaya and A. R. Khokhlov, *Phys. Rev. Lett.*, 1996, **76**, 3029–3031.
- 3 T. T. Perkins, S. R. Quake, D. E. Smith and S. Chu, *Science*, 1994, **264**, 822–825.
- 4 T. T. Perkins, D. E. Smith, R. G. Larson and S. Chu, *Science*, 1995, **268**, 83–87.
- 5 D. E. Smith, T. T. Perkins and S. Chu, *Macromolecules*, 1996, **29**, 1372–1373.
- 6 T. T. Perkins, D. E. Smith and S. Chu, *Science*, 1997, **276**, 2016–2021.
- 7 D. Smith and S. Chu, *Science*, 1998, **281**, 1335–1340.
- 8 D. E. Smith, H. P. Babcock and S. Chu, *Science*, 1999, **283**, 1724–1727.
- 9 C. M. Schroeder, H. P. Babcock, E. S. G. Shaqfeh and S. Chu, *Science*, 2003, **301**, 1515–1519.
- 10 R. M. Jendrejack, E. T. Dimalanta, D. C. Schwartz, M. D. Graham and J. J. de Pablo, *Phys. Rev. Lett.*, 2003, **91**, 038102.
- 11 A. G. Balducci, J. Tang and P. S. Doyle, *Macromolecules*, 2008, **41**, 9914–9918.
- 12 R. M. Robertson and D. E. Smith, *Phys. Rev. Lett.*, 2007, **99**, 126001.
- 13 A. Dambal, A. Kushwaha and E. S. G. Shaqfeh, *Macromolecules*, 2009, **42**, 7168–7183.
- 14 P. G. de Gennes, *Science*, 1997, **276**, 1999–2000.
- 15 C. A. Brockman, S. Kim and C. M. Schroeder, *Soft Matter*, 2010, DOI: 10.1039/C1SM05297G.
- 16 P. G. de Gennes, *Scaling Concepts in Polymer Physics*, Cornell University Press, Ithaca, NY, 1979.
- 17 M. Rubinstein and R. H. Colby, *Polymer Physics*, Oxford University Press, 2003.
- 18 P. C. Hiemenz and T. P. Lodge, *Polymer Chemistry*, CRC Press, 2nd edn, 2007.
- 19 L. J. Fetters, D. J. Lohse, D. Richter, T. A. Witten and A. Zirkel, *Macromolecules*, 1994, **27**, 4639–4647.
- 20 R. G. Larson, *The Dynamics of Complex Fluids*, Oxford University Press, 1999.
- 21 M. Doi and S. F. Edwards, *The Theory of Polymer Dynamics*, Oxford University Press, 1986.
- 22 D. A. McQuarrie, *Statistical Mechanics*, University Science Books, 2nd edn, 2000.
- 23 R. G. Larson, T. T. Perkins, D. E. Smith and S. Chu, *Phys. Rev. E: Stat. Phys., Plasmas, Fluids, Relat. Interdiscip. Top.*, 1997, **55**, 1794–1797.
- 24 B. H. Zimm, *J. Chem. Phys.*, 1956, **24**, 269–278.
- 25 C. M. Schroeder, E. S. G. Shaqfeh and S. Chu, *Macromolecules*, 2004, **37**, 9242–9256.
- 26 R. M. Jendrejack, J. J. de Pablo and M. D. Graham, *J. Chem. Phys.*, 2002, **116**, 7752–7759.
- 27 R. M. Jendrejack, M. D. Graham and J. J. de Pablo, *J. Chem. Phys.*, 2000, **113**, 2894–2900.
- 28 J. F. Marko and E. D. Siggia, *Macromolecules*, 1995, **28**, 8759–8770.
- 29 P. Pincus, *Macromolecules*, 1976, **9**, 386–388.
- 30 O. A. Saleh, D. B. McIntosh, P. Pincus and N. Ribeck, *Phys. Rev. Lett.*, 2009, **102**, 068301.
- 31 D. B. McIntosh, N. Ribeck and O. Saleh, *Phys. Rev. E: Stat., Nonlinear, Soft Matter Phys.*, 2009, **80**, 041803.
- 32 H. J. Choi, S. T. Lim, P.-Y. Lai and C. K. Chan, *Phys. Rev. Lett.*, 2002, **89**, 088302.
- 33 S. Lim, H. Choi and C. Chan, *Macromol. Rapid Commun.*, 2005, **26**, 1237–1240.
- 34 C. M. Schroeder, R. E. Teixeira, E. S. G. Shaqfeh and S. Chu, *Phys. Rev. Lett.*, 2005, **95**, 018301.